A

B
0'00" 1'13" 2'24" 3'36" 4'46"

C
14h 38' 34" 14h 53' 36" 15h 08' 34" 15h 23' 35"

15h 38' 35" 15h 53' 37" 16h 08' 35" 16h 23' 35"

16h 38' 36" 16h 53' 35" 17h 08' 35" 17h 23' 36"
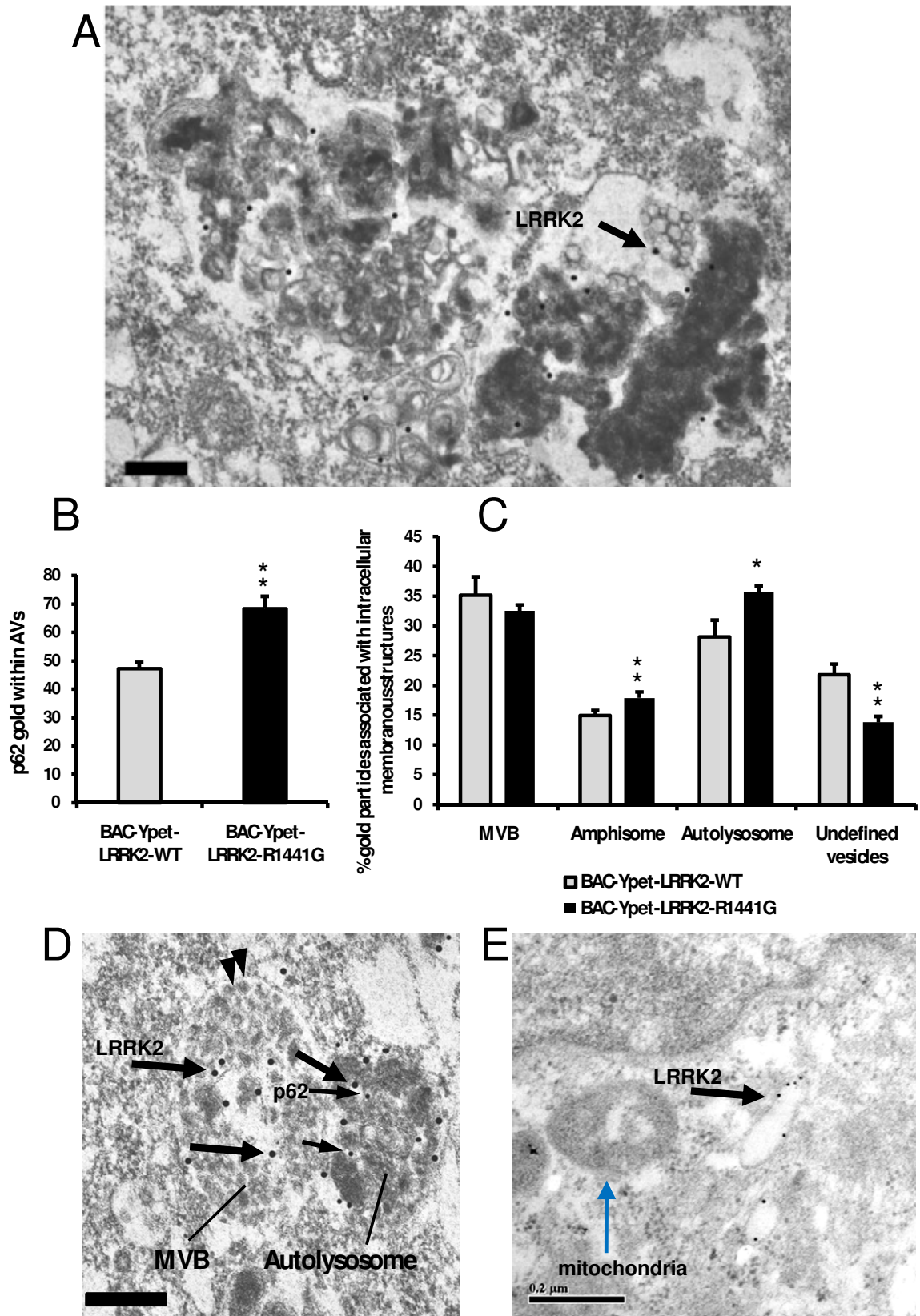
200.00 µm

Figure S1   Alegre-Abarrategui et al.

1

A

LRRK2 →

B

p62 gold within AVs

80
70 **
60
50
40
30
20
10
0

BAC-Ypet-LRRK2-WT   BAC-Ypet-LRRK2-R1441G

C

% gold partides associated with intracellular membranous structures

45
40
35
30
25
20
15
10
5
0

MVB   Amphisome   Autolysosome   Undefined vesicles

□ BAC-Ypet-LRRK2-WT
■ BAC-Ypet-LRRK2-R1441G

D

LRRK2 →
p62 →
MVB   Autolysosome

E

LRRK2 →
mitochondria
0.2 μm

Figure S2   Alegre-Abarrategui et al.

2
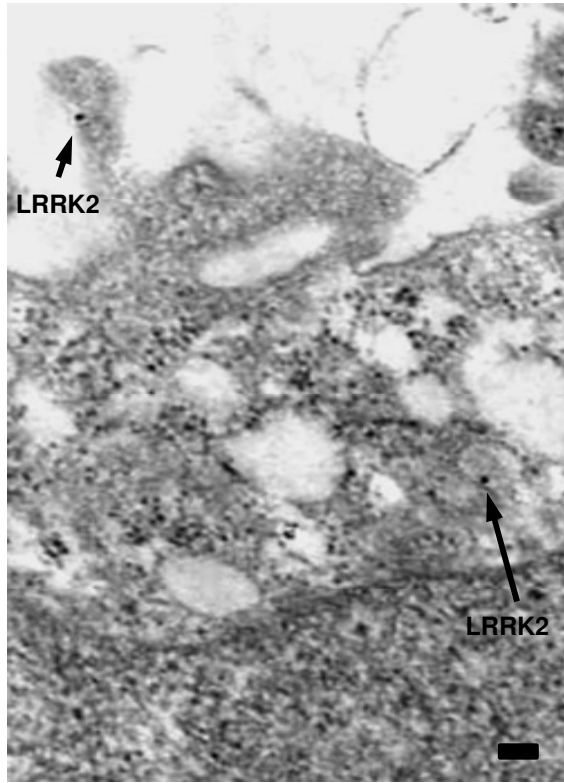
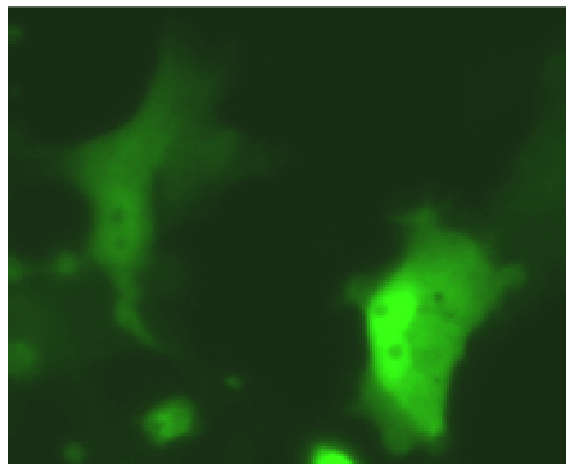Figure S3   Alegre-Abarrategui et al.

Figure S4   Alegre-Abarrategui et al.

SI Figure Legends

Fig. S1. **LRRK2 puncta move towards a paranuclear location.** Cells were transfected with the BAC-YPet-LRRK2-R1441G (A and C) or BAC-YPet-LRRK2-WT (B) and imaged by immunofluorescence (A) or live-cell fluorescence microscopy (B and C). (A) LRRK2 puncta distributed occasionally over a radial pattern with the centre in a paranuclear location. (B) Larger LRRK2 puncta (up to ≈1 µm in diameter), generally lying close to the nucleus, tended to move very little. Smaller puncta (≈0.5 µm or less), however, were highly dynamic and described trajectories in which movement proceed by leaps rather than by smooth, gradual transitions (saltatory movement)(arrows). Speeds of ≈0.5 µm/sec were observed, with a mean speed of ≈0.18 µm/sec. (C) LRRK2 puncta frequently described a net movement towards a paranuclear location when photographed at regular intervals for several hours compatible with the known dynein-mediated transport of MVBs towards the centrosome (1). No difference in speed was observed between WT and mutant.

Fig. S2. **The R1441G LRRK2 pathogenic mutation led to the accumulation of complex AVs containing increased load of p62 and LRRK2.** (A) The R1441G mutation increased the size and complexity of AVs in transfected cells, inducing the formation of complex hybrid organelles of up to 4 µm long containing a mixture of amorphous material, vesicles and incompletely digested darker material. (B) The R1441G mutation led to an accumulation of p62 within AVs as measured by the amount of gold in IEM staining of transfected cells. (C) Upon expression of the R1441G mutation, LRRK2 showed a shift from morphologically-undefined vesicles to AVs, as measured by the total amount of gold per cell in IEM staining of transfected cells using anti-GFP antibodies. (D) IEM photograph of HEK293 cells transfected with BAC-YPet-LRRK2-WT and double labelled with anti-GFP (thick arrows) and p62 antibodies (thin arrows). AVs were double labelled for LRRK2 (GFP) and p62 (organelle on the right displays autolysosome) while MVBs were LRRK2 positive only (organelle on the left). Arrowheads demonstrate that MVBs may simulate to have a double membrane formed by the outer limiting membrane and the membranes of the ILVs. (E) LRRK2 also localised to a lesser extent to morphologically undefined small vesicular structures (arrow). Note that mitochondria (blue arrow) were not labelled. Scale bars represent 500 nm in A and D and 200 nm in E. Counting of all structures was done blind to the genotype. Bars represent mean plus standard error of the mean. Statistical significances were obtained using a Student's *t* test. *p<0.05. **p<0.01.

Fig. S3. **LRRK2 ultrastructural localisation detected with an anti-LRRK2 antibody.** Electron micrograph showing LRRK2 gold labelling on microvilli / filopodia (arrowhead) and intraluminar vesicles of a MVB (arrow) in detached HEH293 cells transfected with BAC-YPet-*LRRK2*-WT and immunolabelled was the anti-LRRK2 antibody EB06550.

Fig. S4. **Untagged YPet expression.** Fluorescence microscopy showing diffuse cytoplasmic and nuclear distribution of untagged YPet expressed from HEK293 cells transfected with pCEP4YPet-MAMM.

SI references

1.   Driskell, O.J., Mironov, A., Allan, V.J. and Woodman, P.G. (2007) Dynein is required for receptor sorting and the morphogenesis of early endosomes, **9,** 113-120.

Supplementary Table 1. Oligonucleotide sequences used in the study

rpsl-neo check_S	GAATTCTCTTTGTTGCTGTTGC
AC107023-BACe3.6_A	GGCCTGGCGGCCGCCTGGCCGTCGACATTTAGGTG ACACTATAGAAGGATCCGCGTTGCACTTTCTTATTGTGG AATGTC
AC084290 3'-pRpsL-neo_S	ACATAATAGAGTTGTTTTTCAACTCTATGTTTGAATGTGGA TACCCTGAATTTTGGGCCTGGTGATGATGGCGGGATC
pRpsl-neo_BACe3.6_A	GGCCTGGCGGCCGCCTGGCCGTCGACATTTAGGTG ACACTATAGAAGGATCCGCGTCAGAAGAACTCGTCA AGAAGG
OH-N-YPetwtHR_S_S	GAGCAGCGGACGTTCATGCTGGGAGGGCGGCGG GTTGGAAGCAGGTGCCACCATGGTGAGCAAAGGC GAAGAGCTGTTC
P-N-YPetwtHR_A_S	CCTTCTTGACGAGTTCTTCTGACCTGACCGCCGCCGG CATCACCGAGGGCATGAACGAGCTCTATAAGGGAG CTGGAG
OH-N-YPetwtHR_A_A	AACTTCTTCAGAGTTTCCTCGTCCTCTTCGCACCCCTGA CAGCTGCCACTAGCTCCAGCTCCAGCTCCCTTATAG AGCTC
P-N-YPetwtHR_S_A	GATCCCGCCATCATCACCAGGCCGTCCAGCTCCAC CAGGATGGGCACCACGCCGGTGAACAGCTCTTCG CCTTTGCTCAC
OH-GFPwtHRbis_S_S	GGTGAGCTGAGCTCGCCCCCGGGGAGCTGTGGCC GGCGCCCCTGCCGGTTCCCTGAGCAGCGGACGTT CATGCTGGGAGG

P-N-MYPetwtHRbis_S_A	CAGCTCTTCGCCTTTGCTCACCATGGTGGCACCTGCTTCCAACCCGCCGCCCTCCCAGCATGAACGTCCGC
P-N-MYPetwtHRbis_A_S	GGGCATGAACGAGCTCTATAAGGGAGCTGGAGCTGGAGCTAGTGGCAGCTGTCAGGGGTGCGAAGAGGACGAGGAAACTC
OH-N-EmGFPwtHRbis_A_A	GCGTTTCTATCTGTTTTCCTTCCTGGACATTGTTCAGCCTGACTATCAACTTCTTCAGAGTTTCCTCGTCCTCTTCGCAC
G2019S EcoRI_S	GCTGCAGGAATTCAAGGGACAAAGTGAGCACAG
G2019S XhoI_A	GCCCCCCCTCGAGTTTTTGCCCTGAAAAATTACATC
R1441G EcoRI_S	GCTGCAGGAATTCAAGGCATGAAGATGGGAAAG
R1441G XhoI_A	GCCCCCCCTCGAGTGATGGTTTTCCGAAGTTTTG
G2019S SDM_S	GCAAAGATTGCTGACTACAGCATTGCTCAGTACTG
G2019 SDM_A	GCAGTACTGAGCAATGCTGTAGTCAGCAATCTTTGC
R1441G SDM_S	GTCTTTCCCTCCAGGCTTGCGCTTCTTCTTCCCCTG
R1441G SDM_A	CAGGGGAAGAAGAAGCGCAAGCCTGGAGGGAAAGAC
RpSL G2019S_S	GCTGCTTTTCACACTGTATCCCAATGCTGCCATCATTGCAAAGATTGCTGACTACGGCCTGGTGATGATGGCGGGATC
RpSL G2019S_A	CCTGGTGTGCCCTCTGATGTTTTTATCCCCATTCTACAGCAGTACTGAGCAATGCTCAGAAGAACTCGTCAAGAAGG
RpSL R1441G_S	GCAGGCCCAGTTTGAAAGCAAACACAAGAGGGTTTTGTGTCTTTCCCTCCAGGCTGGCCTGGTGATGATGGCGGGATC
RpSL R1441G_A	TCATCAGAAACATCCAAATGTGTGCCAACGAGAATCACAGGGGAAGAAGAAGCGCTCAGAAGAACTCGTCAAGAAGG
G2019S_S	AAGGGACAAAGTGAGCACAG
G2019S_A	TTTTTGCCCTGAAAAATTACATC
R1441G_S	AAGGCATGAAGATGGGAAAG
R1441G_A	TGATGGTTTTCCGAAGTTTTG

SP AC084290 at -10Kb	GCGTATTGCCTACAAAAACC
ASP AC084290 at -10Kb	AGCAGCTTGCACAACCTTTC
SP for AC084290 MIDDLE	TTCCCAATCTATTCAAGGATCAG
AC084290 3' 1KB_S	TGCTTAAGACAGGACTATTGCTTG
AC084290 3' 1KB_A	GCATCACAAATTTAGGGAAAAG
AC084290 3' end_S	GAATGTGGATACCCTGAATTTTG
pBACe3.6 5'end_A	TTGATGTTCATGTTCATGTCTCC
pBACe3.6 3'end_S	AGGACTATATTGCTCTAATAAATTTGC
AC084290 5'end_A	GGATGGGTAGTTGGCAGAAG